Cell Reports
Physical Science

CellPress
OPEN ACCESS

Article

A reusable soy protein adhesive with enhanced weather resistance through construction of a cutin-like structure

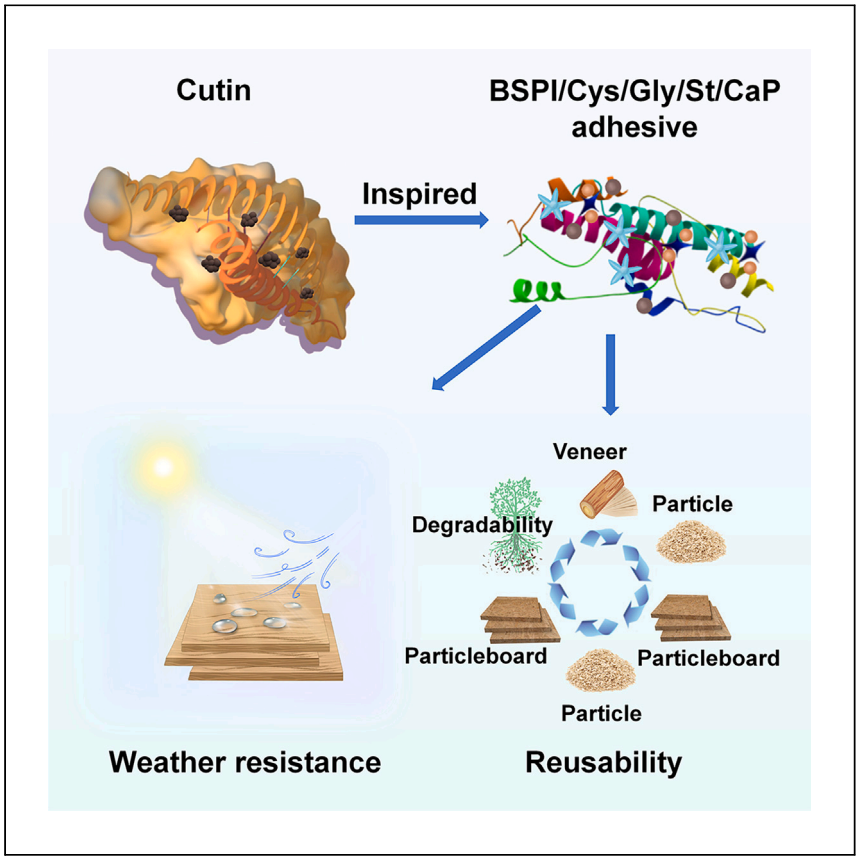

Huang et al. present a groundbreaking soy protein adhesive inspired by animal cutin, which shows remarkable weather resistance and reusability. Its potential to replace harmful synthetic resin adhesives aligns with sustainable development and environmental protection goals, signifying a major advancement in durable plant-protein-based adhesives.

Xinxin Huang, Yanqiu Chen, Xixiang Lin, ..., Jianzhang Li, Qiang Gao, Pingan Song

gaoqiang@bjfu.edu.cn (Q.G.)
pingan.song@usq.edu.au (P.S.)

Highlights

A soy protein adhesive with exceptional weather resistance as phenolic resin

The adhesive exhibits excellent reusability and can reprocess wood-based panels

The adhesive displays excellent bonding performance and can bond various substrates

The adhesive also has mold resistance, flame retardancy, and eco-friendliness

Huang et al., Cell Reports Physical Science 5, 102024
June 19, 2024
https://doi.org/10.1016/j.xcrp.2024.102024

Cell Reports
Physical Science

CellPress
OPEN ACCESS

Article

A reusable soy protein adhesive with enhanced weather resistance through construction of a cutin-like structure

Xinxin Huang,[1] Yanqiu Chen,[1] Xixiang Lin,[1] Jingchao Li,[1] Jing Luo,[2] Jianzhang Li,[1] Qiang Gao,[1,5,*] and Pingan Song[3,4,*]

SUMMARY

Enhancing the weather resistance and reprocessability of soy protein-based (SP) adhesives poses a considerable challenge. Here, we report an SP adhesive inspired by animal cutin, featuring dynamic covalent bonds and an organic-inorganic hybrid structure. The soy protein isolate undergoes enzymatic hydrolysis and is then combined with L-cysteine, which is subsequently grafted with glycidol and sodium tetraborate to create disulfide bonds and borate ester bonds, along with mineralized calcium phosphate. This adhesive effectively bonds various substrates, enabling stainless-steel sheets to pull a 1,135 kg car. Additionally, the adhesive exhibits remarkable weather resistance comparable to a phenolic resin (PF) adhesive in an accelerated aging test. It showcases outstanding reusability, surpassing commercial urea-formaldehyde resins and PF adhesives in particleboard reprocessability. Furthermore, the adhesive proves to be mildew resistant, flame retardant, degradable, and eco-friendly. This study signifies a significant advancement in reusable and weather-resistant adhesives derived from plant proteins.

INTRODUCTION

Adhesives, polymers utilized to bond materials together, have broad applications in various fields, such as biomedicine, electronics, aerospace, and architecture.[1–3] Synthetic resin adhesives are commonly used due to their robust adhesion and easy curing.[4,5] However, their reliance on non-renewable petroleum resources and emission of harmful volatiles pose significant environmental and health hazards.[6,7] Hence, there is a growing interest in exploring renewable natural substances as substitutes for synthetic resins. Soy protein-based (SP) adhesives, which are renewable, easily accessible, and biodegradable, offer considerable potential for development.[8,9] These adhesives are extensively employed in wood processing for manufacturing furniture plywood and joinery board products. Through modification techniques, the water resistance,[10,11] mold resistance,[12] coating properties,[13,14] and prepressing characteristics[15] of SP adhesives have been enhanced, enabling the creation of engineered wood products for indoor use. Engineered wood products provide benefits such as renewability, environmental compatibility, and ease of mass production. With the increasing recognition of wood-based composites as sustainable alternatives to metals and polymers, there is growing demand for their extension beyond indoor environments. However, to expand their applications, it is essential to tackle challenges related to weather resistance and reprocessability of wood-based composites. Enhancing these aspects is vital for efficient

[1]State Key Laboratory of Efficient Production of Forest Resources, Ministry of Education & Beijing Key Laboratory of Wood Science and Engineering, Beijing Forestry University, Beijing 100083, China

[2]College of Materials Science and Engineering, Nanjing Forestry University, Longpan Road 159, Xuanwu District, Nanjing 210037, China

[3]Centre for Future Materials, University of Southern Queensland, Springfield, QLD 4300, Australia

[4]School of Agriculture and Environmental Science, University of Southern Queensland, Springfield, QLD 4300, Australia

[5]Lead contact

*Correspondence: gaoqiang@bjfu.edu.cn (Q.G.), pingan.song@usq.edu.au (P.S.)

https://doi.org/10.1016/j.xcrp.2024.102024

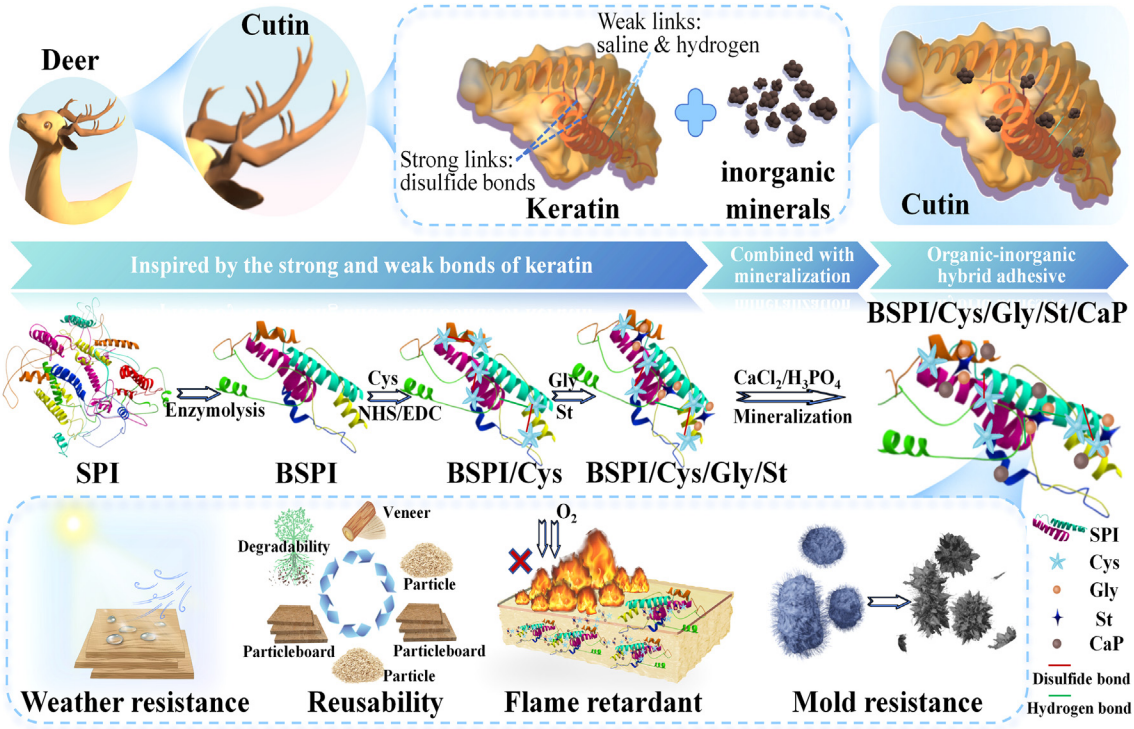

Figure 1. Preparation process and key properties of the BSPI/Cys/Gly/St/CaP adhesives

waste management from engineered wood products, conservation of wood resources, improved wood recycling, and reduced carbon emissions to achieve sustainable development. Nevertheless, soy protein, a natural material, exhibits inadequate weather resistance, rendering it susceptible to outdoor temperature fluctuations and humidity variations. This leads to decreased adhesive performance and premature aging. Furthermore, the crosslinked modification of soy protein impairs its reusability, hindering its potential as a reusable adhesive.[16] Developing a weather-resistant and reusable soy protein adhesive presents significant challenges.

Animal cutin, primarily composed of keratin and a modest amount of inorganic minerals, exhibits exceptional weather resistance and stability.[17] The abundant amino acid composition of keratin, notably cysteine content,[18] facilitates the formation of durable disulfide crosslinks, enhancing its stability.[19] Additionally, the interaction between keratin and inorganic minerals reinforces the strength, hardness, and durability of animal cutin.[20] Leveraging the structure and composition of keratin and its composites with inorganic minerals to enhance the weather resistance of SP adhesives represents a promising advancement.

In this study, an SP adhesive is formulated utilizing soy protein isolate (SPI), L-cysteine (Cys), glycidol (Gly), sodium tetraborate (St), and mineralized calcium phosphate (CaP). By incorporating dynamic covalent bonds and mineralized inorganic materials into the SP adhesive system, cutin-like composites are created (Figure 1), enabling the SP adhesive to exhibit three significant advantages. Firstly, it demonstrates exceptional weather resistance comparable to phenolic resin (PF) adhesives in an accelerated aging test. Secondly, it showcases outstanding reusability, with an average residual rate of approximately 84% after five cycles, along with the capacity of the adhesive film and particleboard to be reprocessed. The

particleboard maintains a modulus of elasticity (MOE) and a modulus of rupture (MOR) of 2,395.31 and 13.95 MPa, respectively, surpassing the requirements for P2 particleboards (furniture particleboards for interior use) even after two cycles. Finally, the adhesive exhibits remarkable versatility, including high bonding strength, excellent mildew resistance (extending beyond 17 days for liquid adhesives), flame retardancy (adhesive's limiting oxygen index of 30.6%), superior degradability, and eco-friendliness. These features position the developed SP adhesive as a highly promising alternative to conventional weather-resistant disposable adhesives in engineering applications.

RESULTS AND DISCUSSION

Formation and physicochemical characterization of SP adhesives

The synthetic route of the SP adhesive with a dynamic covalent network and an organic-inorganic hybrid structure is depicted in Figure S1. Bromelain was utilized to enhance the soy protein's reactivity and expose more active groups, resulting in bromelain-hydrolyzed SPI (BSPI). The incorporation of thiol groups into the SPI chains was achieved through amidation reactions with BSPI by incorporating Cys. Additionally, Gly and St were introduced to improve the bond strength and reusability of the adhesives. After the ring-opening reaction between the epoxy group of Gly and the amino group, carboxyl group, and hydroxyl group of BSPI, it was exposed that the dihydroxyl group formed borate bonds with St, which provided another dynamic covalent bond for the adhesive. The organic-inorganic hybrid adhesive was constructed through the mineralization of micro-nano CaP using calcium chloride ($CaCl_2$) and phosphoric acid (H_3PO_4).

The molecular weight of BSPI decreased from 3,067 to 1,738 g/mol, and the polydispersity decreased from 2.043 to 1.483 (Figure 2A). The viscosity of the BSPI adhesive decreased from 34,150 to 27,710 mPa s (Figure 2B), and the contact angle decreased from 68.7° to 62.4° (Figure 2C). Decreasing the molecular weight of soy protein and exposing more active groups are beneficial for subsequent modification. However, excessive enzymatic hydrolysis leading to the conversion of proteins into amino acids can significantly impact the bonding performance of the SP adhesive. Therefore, controlled enzymatic hydrolysis was achieved by controlling the reaction endpoint through high-temperature inactivation, as well as by observing the viscosity and determining the molecular weight.

The introduction of Cys into BSPI was confirmed by the appearance of new peaks at 1,345 and 774 cm^{-1} in the attenuated total reflectance-Fourier transform infrared (ATR-FTIR) spectrum (Figure 2D), corresponding to the stretching bands of C–N–C[21] and C–S,[22] respectively. Fourier self-deconvolution of the ATR-FTIR data was conducted to analyze the changes in secondary structures after the amidation reaction (Figures 2E and 2F). The relative contents of the β-sheet and random coils in BSPI/Cys significantly increased compared to BSPI, while the relative contents of the β-turn and α-helix decreased. These findings indicate that the introduction of Cys successfully reorganized the polypeptide chain (BSPI) through amide bonds, resulting in alterations in the secondary structure of BSPI.

The incorporation of Gly into the BSPI/Cys adhesive was confirmed by the appearance of a new ester bond peak at 1,735 cm^{-1} and a decrease in the amide II (N-H) peak at 1,529 cm^{-1} in the ATR-FTIR spectrum (Figure 2D), suggesting the reaction between the epoxy groups on Gly and the carboxyl and amino groups on BSPI. The ultraviolet-visible (UV-vis) spectra (Figure 2G) demonstrated a redshift of the

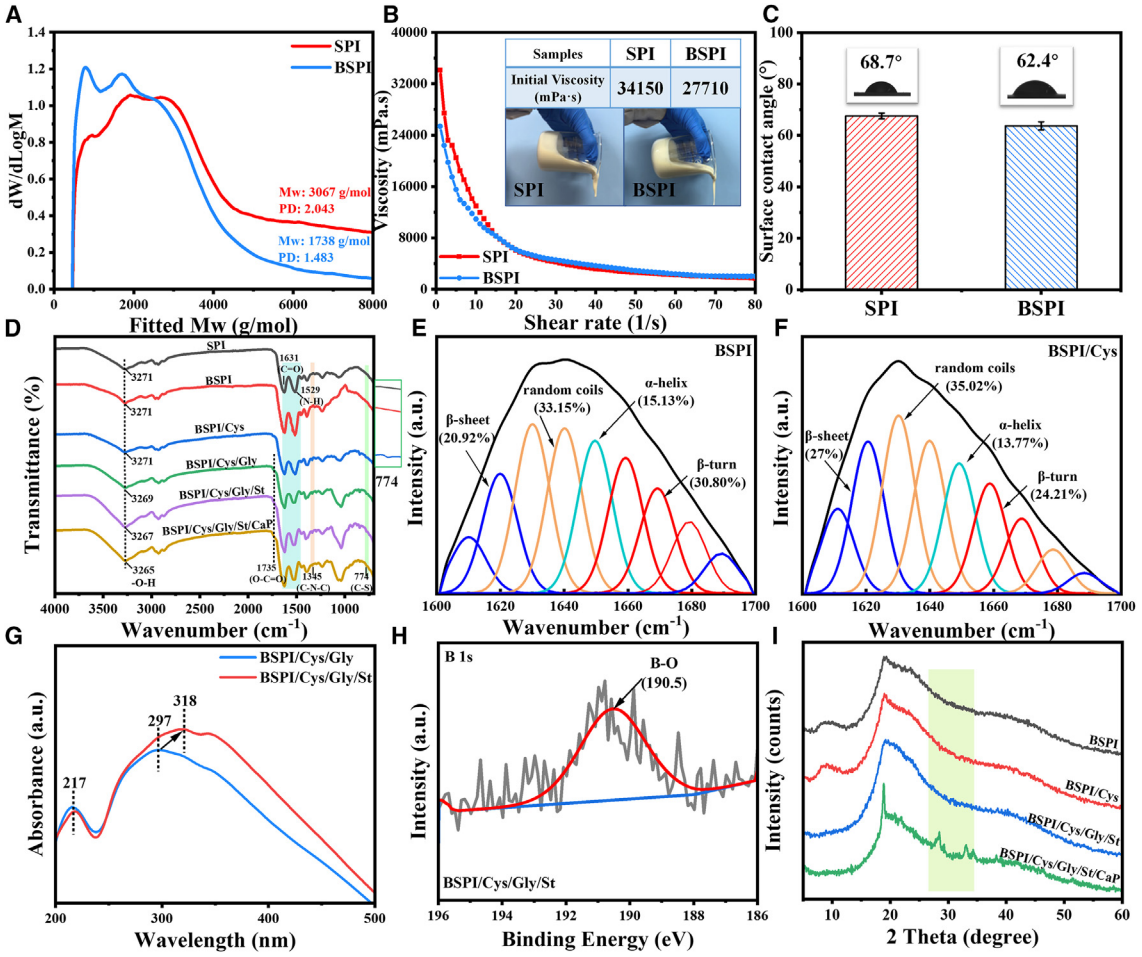

Figure 2. Formation and physicochemical characterization of SP adhesives

(A–C) Gel permeation chromatography curves, viscosity, and surface contact angle of SPI and BSPI adhesives (ANOVA, $N = 6$ for each treatment, $p < 0.05$).

(D) ATR-FTIR spectra of the cured SP adhesives.

(E and F) ATR-FTIR spectra deconvolution and peak assignment of BSPI and BSPI/Cys adhesives.

(G) UV-vis absorption spectra of BSPI/Cys/Gly and BSPI/Cys/Gly/St adhesives.

(H) B 1s XPS spectra of the BSPI/Cys/Gly/St adhesive.

(I) XRD spectra of SP adhesives.

characteristic peaks of BSPI/Cys/Gly (from 297 to 318 nm) upon the addition of St. Furthermore, the B 1s X-ray photoelectron spectroscopy (XPS) spectrum of dialyzed BSPI/Cys/Gly/St adhesive exhibited a peak at 190.5 eV attributed to B–O bonds (Figure 2H).[23] This suggests the formation of borate ester bonds through the complexation of St with the exposed Gly diols after ring opening.[24,25] X-ray diffraction (XRD) analysis revealed the successful preparation of CaP, as the mineral intermediate phase exhibited a broad diffraction peak (Figure 2I), confirming its amorphous characteristic.[26]

Bonding performance of the SP adhesives

The bonding performance of SP adhesives in three-ply plywood bonding was evaluated through dry and wet shear strength measurements (Figure S2). The BSPI/Cys/Gly/St/CaP adhesive exhibited significant improvements in both dry and wet shear strength, with values of 2.18 and 1.08 MPa, respectively. This represented a 31.33%

increase in dry shear strength and a 107.69% enhancement in wet shear strength compared to the SPI adhesive (1.66 and 0.52 MPa, respectively). The performance of the BSPI/Cys/Gly/St/CaP adhesive surpassed that of commercial urea-formaldehyde resins (UFs)[27] and various biobased adhesives, including SP,[28–30] peanut meal-based,[31] tannin-based,[32] lignin-based,[33] and starch-based adhesives[34] (Figure S3). Scanning electron microscopy (SEM) image analysis revealed that the cross-section of the BSPI/Cys/Gly/St/CaP adhesive appeared denser and smoother compared to SPI, BSPI, and BSPI/Cys adhesives (Figure S4), indicating an increased crosslinking density attributed to the incorporation of disulfide and borate ester bonds, which improved resistance against water infiltration. Energy-dispersive X-ray spectroscopy (EDS) analysis confirmed the uniform distribution of CaP within the adhesive network without any phase separation or particle aggregation.[35]

The potential of the BSPI/Cys/Gly/St/CaP adhesive as a universal adhesive for various substrates such as glass, aluminum (Al), stainless steel (SS), wood, and their combinations was explored using a lap shear test (Figure S5). As shown in Figure 3A, the average bond strengths of the adhesive on different substrates were determined: wood (1.44 MPa), glass (0.8 MPa), Al (0.89 MPa), and SS (1.57 MPa). Glass, forming only hydrogen bonds with the adhesive,[36,37] exhibited the lowest bond strength, while wood, providing both hydrogen bonds and mechanical interlocking, showed higher bond strength. The highest bond strength on SS was attributed to the enzymatic hydrolysis of soy protein, exposing more reactive groups that could coordinate with metal ions on the SS surface. The lower bond strength on Al was due to surface oxidation effects[25] (Figure 3B). To further elucidate the adhesion mechanism of the adhesive, molecular dynamics (MD) simulations were utilized to evaluate the adhesive properties of BSPI/Cys/Gly/St/CaP adhesive molecules on glass and SS substrates. The interfacial adhesion energy ($E_{adhesion}$) represents the interaction energy between the adhesive and the adherend substrate, while the cohesion energy ($E_{cohesion}$) indicates the interaction energy among the adhesive molecules. At 25°C, the $E_{adhesion}$ values of BSPI/Cys/Gly/St/CaP on SS and glass surfaces were −5,435,860 and −2,407,164 kcal mol^{-1}, respectively, as depicted in Figure 3C. This could be attributed to the interaction between different substrates and adhesive molecules, leading to changes in the conformation of the adhesive molecules, including adjustments in bond angles, bond lengths, and other structural aspects. Moreover, the $E_{adhesion}$ of BSPI/Cys/Gly/St/CaP on SS was calculated to be −9,171,983 kcal mol^{-1}, exceeding that of glass (−5,843,024 kcal mol^{-1}), suggesting a higher interfacial adhesion force of BSPI/Cys/Gly/St/CaP on SS, consistent with lap shear test results. Additionally, the $E_{adhesion}$ of BSPI/Cys/Gly/St/CaP on the SS surface significantly exceeded the $E_{cohesion}$, indicating that bond strength is primarily governed by cohesion. Furthermore, the bond strength of the adhesive without bromelain enzymatic hydrolysis (SPI/Cys/Gly/St/CaP) was lower than that of the BSPI/Cys/Gly/St/CaP adhesive, emphasizing the significance of the hydrolysis step (Figure S6). This is mainly due to the decrease in the molecular weight of soy protein during bromelain enzymatic hydrolysis, facilitating easier penetration into micro-defects and voids on the surface of the adherend during the bonding process, thereby enhancing the physical anchoring effect. Additionally, enzymatic hydrolysis exposes more reactive groups, such as carboxyl and amino groups, which boost the reactivity of soy protein, resulting in higher bond strength.

The stability of the adhesive was evaluated through knocking and dropping tests on glass, a challenging substrate for bonding. The BSPI/Cys/Gly/St/CaP adhesive demonstrated excellent impact stability, exhibiting no failure (Figure 3D; Videos S1, S2, and S3). Furthermore, the long-term bond strength (>90 days) of the

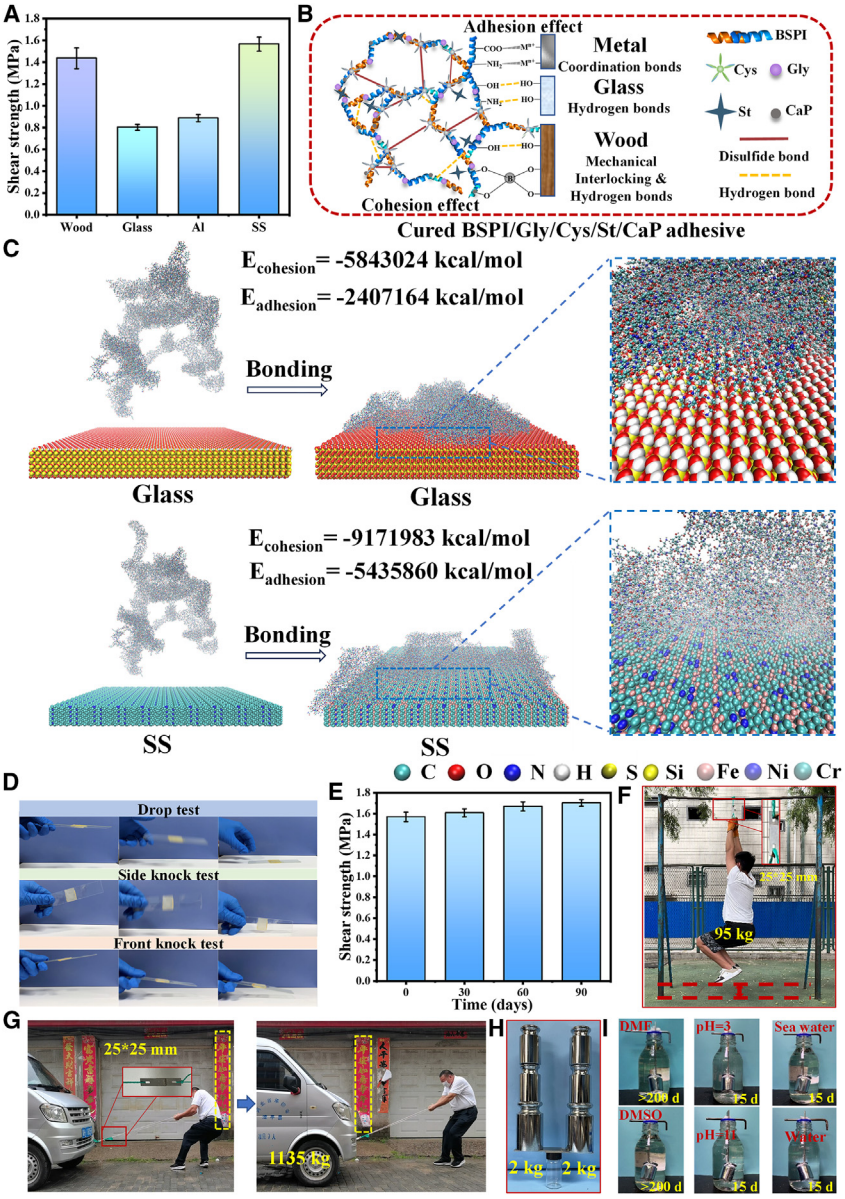

Figure 3. Bonding performance of the SP adhesives

(A and B) Shear strength (A) and bonding mechanism (B) of the BSPI/Cys/Gly/St/CaP adhesive (ANOVA, $N = 6$ for each treatment, $p < 0.05$).

(C) The BSPI/Cys/Gly/St/CaP adhesive adhered to the SS and glass at 25°C.

(D) Stability tests of the glass sheet bonded with BSPI/Cys/Gly/St/CaP adhesive, including drop test, side knock test, and front knock test.

(E) Long-term shear strength test of the BSPI/Cys/Gly/St/CaP adhesive-bonded SS sheet (ANOVA, $N = 6$ for each treatment, $p < 0.05$).

(F–H) Photos of the BSPI/Cys/Gly/St/CaP adhesive-bonded SS sheet (bonded area, 25 × 25 mm) to (F) support a 95 kg adult male, (G) drag a 1,135 kg car, and (H) carry a weight of 2 kg at both ends.

(I) Weight (500 g) immersed in multiple conditions.

adhesive on SS substrates was assessed (Figure 3E). SS sheets bonded by the BSPI/Cys/Gly/St/CaP adhesive displayed exceptional bond strength in various scenarios, such as lifting a 95 kg adult male (Figure 3F; Video S4), pulling a car weighing 1,135 kg (Figure 3G; Video S5), and supporting a 2 kg weight at both ends

(Figure 3H). To demonstrate the versatility of the adhesive, bonded SS sheets were subjected to various conditions including water, artificial seawater, organic solvents (N, N-dimethylformamide, dimethyl sulfoxide), alkaline solution (pH = 11), and acidic solution (pH = 3). The SS sheets bonded by the adhesive suspended a weight of 500 g for over 200 days in organic solvents and 15 days in aqueous solvents (Figure 3I), underscoring the effectiveness of the dynamic covalent bond system and the organic-inorganic hybrid structure in enhancing water resistance.

The weather resistance of the SP adhesives

The weather durability of adhesive-bonded wood products is crucial for their long-term service life. To evaluate the weather resistance of the BSPI and BSPI/Cys/Gly/St/CaP adhesives, accelerated aging and wet-hot aging tests were conducted. ATR-FTIR analysis was used to assess the chemical structure changes of the adhesives under different aging conditions (Figures 4A and 4B). Accelerated aging treatment (A) resulted in a reduced intensity of characteristic absorption bands associated with soy protein in the untreated (S) BSPI adhesive, such as the C=O stretching vibration (amide I) and N-H bending vibration (amide II). Additionally, the absence of the C-N peak at 1,312 cm^{-1} suggests changes in the stability of its structural groups in the BSPI adhesive.[38] However, the influence of wet-hot aging treatments at 50°C and 70°C on the BSPI adhesive was minimal. In contrast, the characteristic peaks of the BSPI/Cys/Gly/St/CaP adhesive after accelerated aging and wet-hot aging treatments showed insignificant changes, suggesting better weather resistance for this adhesive. To further evaluate weather resistance, thermogravimetric (TG) analysis was performed on the adhesives subjected to accelerated aging and wet-hot aging (Figures 4C and 4D). The BSPI adhesive exhibited a high mass thermal loss rate of 74.23% due to its physical entanglement of protein molecules and lower degree of crosslinking. However, after the 70°C wet-hot aging treatment, the mass thermal loss of the BSPI adhesive was reduced, indicating its improved stability due to enhanced intermolecular interactions and crosslinking structures. Particularly, the mass thermal loss rate of the BSPI/Cys/Gly/St/CaP adhesive remained relatively stable and lower than that of the BSPI adhesive after aging treatment, suggesting superior weather resistance.

The effect of the aging treatment on the bond strength of plywood specimens prepared with the BSPI and BSPI/Cys/Gly/St/CaP adhesives was also investigated (Figures 4E and 4F). The bond strength of both plywood specimens decreased after artificial accelerated aging. Under the BS1 aging conditions, the bond strength of the plywood specimens prepared with BSPI and BSPI/Cys/Gly/St/CaP adhesives decreased the most, by 65.77% and 36.71%, respectively. Similarly, under the BS2 aging conditions, after three cycles of soaking, freezing, and drying, the bond strength of the plywood specimens decreased by 46.98% and 18.84%, respectively. These results indicate that the weather resistance of plywood prepared with the BSPI/Cys/Gly/St/CaP adhesive significantly improved. To further compare the weather resistance, commercial PF and UF adhesives were selected as controls. Plywood specimens prepared with these adhesives were subjected to three cycles of GB4-10 aging conditions (Figures 4G–4I). After three cycles, the UF-bonded plywood exhibited no bond strength, while the bond strengths of BSPI/Cys/Gly/St/CaP- and PF-bonded plywood are 0.77 and 0.85 MPa, respectively. Residual rate tests conducted after three cycles of GB4-10 aging also confirmed the superior weather resistance of the BSPI/Cys/Gly/St/CaP adhesive (Figures 4J–4L), with a residual rate of 44.06%, compared to the PF adhesive (49.1%) and the complete dissolution of the UF adhesive. These findings highlight that the BSPI/Cys/Gly/St/CaP adhesive demonstrates excellent weather resistance comparable to PF adhesives and superior to UF adhesives.

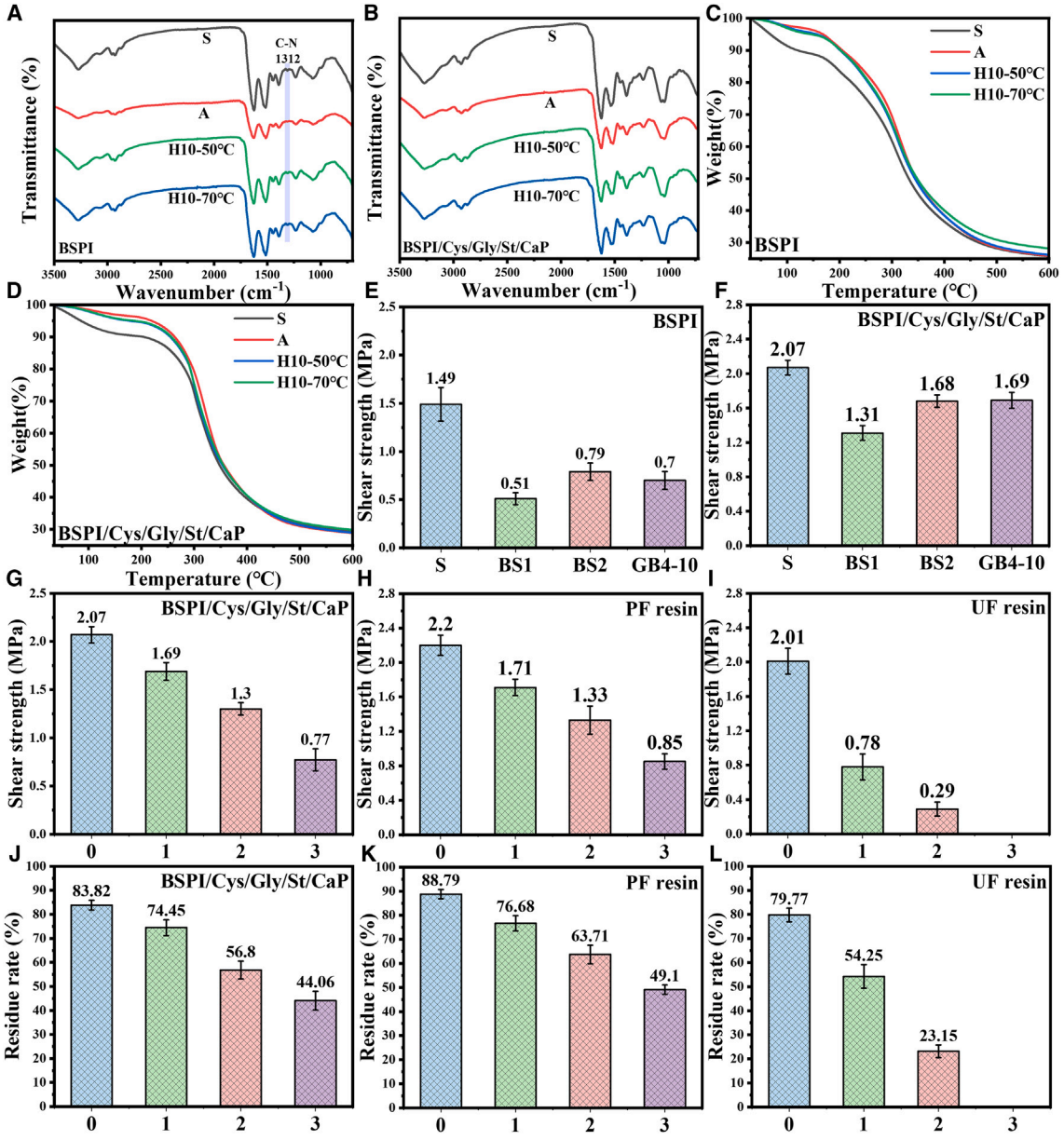

Figure 4. The weather resistance of the SP adhesives

(A–D) ATR-FTIR spectra (A and B) and TG spectra (C and D) were conducted on both untreated BSPI and BSPI/Cys/Gly/St/CaP adhesives (S) and those that underwent accelerated aging (A) and wet-hot aging treatments (H10-50°C, H10-70°C).

(E and F) Shear strength of wood bonded with BSPI and BSPI/Cys/Gly/St/CaP adhesives after accelerated aging tests (ANOVA, $N = 6$ for each treatment, $p < 0.05$).

(G–I) Shear strength comparison of wood bonded with BSPI/Cys/Gly/St/CaP, UF, and PF adhesives after three cycles of accelerated aging using the GB4-10 method (ANOVA, $N = 6$ for each treatment, $p < 0.05$).

(J–L) Residual rate of BSPI/Cys/Gly/St/CaP, UF, and PF adhesive powders after three cycles of accelerated aging (ANOVA, $N = 6$ for each treatment, $p < 0.05$).

Reusability of BSPI/Cys/Gly/St/CaP adhesive and reprocessability of wood-based panels

The achievement of reusability in thermosetting adhesives, such as SP adhesives, is of utmost importance for enhancing the sustainability of applications. This includes minimizing material waste, reducing environmental impact, and improving cost

effectiveness and resource efficiency in various industries. In this study, the residual rate of the cured BSPI/Cys/Gly/St/CaP adhesive was investigated through multiple cycles of grinding, hot pressing into films, and regrinding into powder (Figure 5A). The results exhibited consistent residual rates of approximately 84% for the adhesive powder, even after undergoing five cycles (Figure 5B). These rates surpassed those reported in the literature for other SP adhesives (Figure S7). Additionally, the reusability of the adhesive was confirmed by preparing BSPI/Cys/Gly/St/CaP films using the same raw material ratios (Figure 5C). Even after cutting the film into pieces and subjecting it to hot pressing, a new film could still be formed, with the tensile strength and elastic modulus remaining above 60% after two cycles (Figure 5D). These findings indicate that the dynamic covalent bonds formed in the adhesive undergo rearrangement during each hot-pressing cycle, enabling its reusability. Notably, the adhesive powder transformed directly into a film after hot pressing, and heating of the film did not cause melting (Video S6). This observation suggests that the adhesive remains a thermosetting adhesive and the change in form can be attributed to the rearrangement of dynamic covalent bonds. To determine the specific temperature and pressure required for the rearrangement of dynamic covalent bonds in the BSPI/Cys/Gly/St/CaP adhesive during hot pressing, cured adhesive powder with a moisture content of 20% was coated on an SS sheet and dried under varying temperatures for 2 h. It was observed that the shear strength of the SS sheets increased from 60°C to 140°C. However, considering the minimal difference in shear strength at 120°C and 140°C, and in the interest of ensuring the bonding quality and cost effectiveness and minimizing energy consumption, a temperature of 120°C was chosen as the optimal reaction. It is worth noting that the shear strength of SS sheets remained relatively low throughout the temperature increase (Figure 5E), emphasizing the significance of pressure for the rearrangement of dynamic covalent bonds during the hot-pressing process. Subsequently, increasing the hot-pressing pressure from 1 to 5 MPa at 120°C initially increased and then decreased the shear strength of the SS sheets bonded with the BSPI/Cys/Gly/St/CaP adhesive powder, reaching its maximum value at 3 MPa (Figure 5F). The increase in the contact area between the SS sheets and the adhesive powder under rising pressure was found to facilitate better physical contact, promoting the formation of a uniform adhesive layer and enhancing the shear strength. However, excessive pressure caused material compression, generating significant internal stress that affected adhesion negatively. Consequently, the optimal conditions for the rearrangement of dynamic covalent bonds in the BSPI/Cys/Gly/St/CaP adhesive during hot pressing were determined to be 120°C and 3 MPa.

In addition to reusability, it is also crucial to achieve the reprocessability of wood-based panels using the SP adhesive as a wood adhesive. In this regard, poplar wood particles and BSPI/Cys/Gly/St/CaP adhesives were hot pressed to create first-generation particleboards. Subsequently, only deionized water (without reglu-ing) was applied to produce second- and third-generation particleboards (Figure 5G). The first-generation particleboard displayed high MOE and MOR values of 3,133.05 and 19.25 MPa, respectively. Even after one cycle, the MOE and MOR values of the second-generation particleboard accounted for 92.95% and 93.71% of the values exhibited by the first-generation particleboard, respectively. After two cycles, the MOR and MOE of the third-generation particleboard still reached 76.45% (2,396.31 MPa) and 72.47% (13.95 MPa) of the original values, respectively (Figures 5H and 5I). These retained values comply with the requirements specified for P2-type particleboards as per GB/T 4897-2015, where MOR $\geq$ 11 MPa. The decline in mechanical properties after two cycles can be attributed to the fact that the wood particles in the particleboard approach a powdered state (Figure S8). In

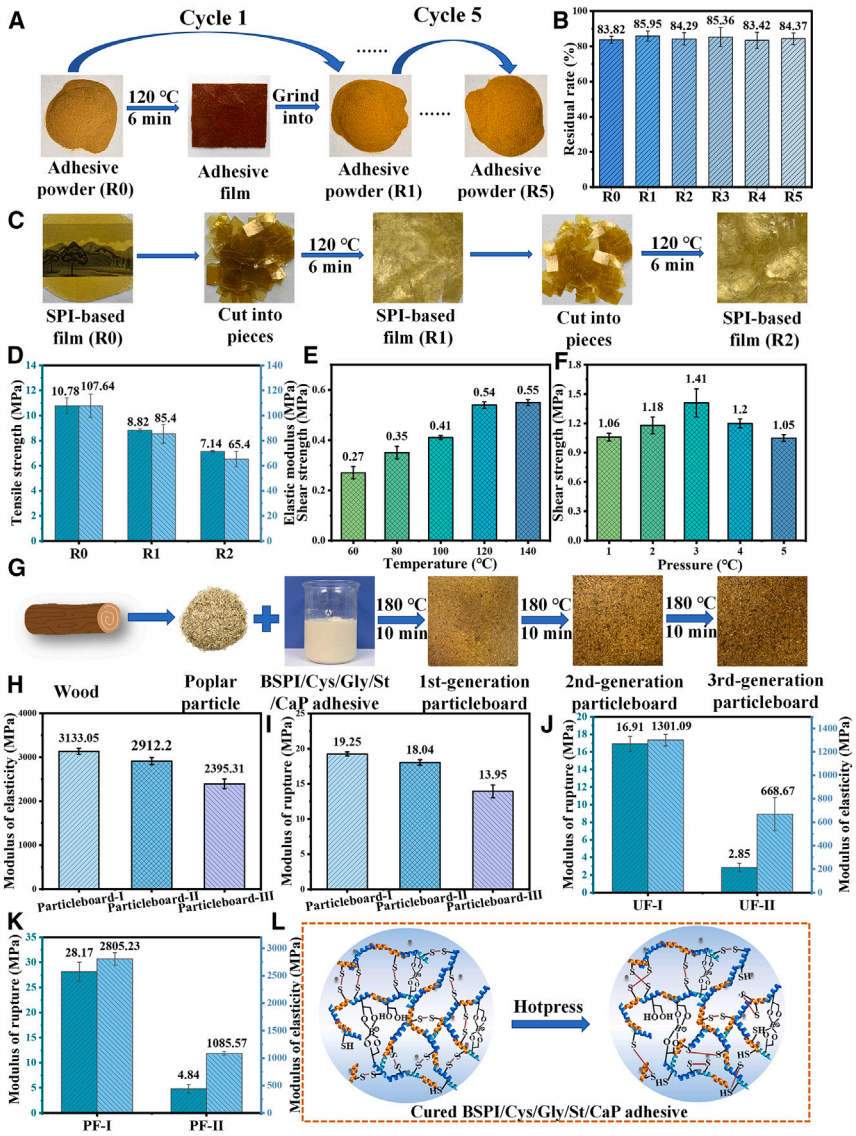

Figure 5. Reusability of BSPI/Cys/Gly/St/CaP adhesive and reprocessability of wood-based panels

(A) Schematic representation of the cycling test for residual rate evaluation of adhesive powder.

(B) Residual rate of adhesive powder after undergoing five cycles of hot pressing (ANOVA, $N = 6$ for each treatment, $p < 0.05$).

(C) Schematic illustration of the recyclability of SPI-based film.

(D) Tensile strength and elastic modulus of the SPI-based film after two cycles (ANOVA, $N = 6$ for each treatment, $p < 0.05$).

(E and F) Shear strength of SS sheets bonded under different temperatures and pressures (ANOVA, $N = 6$ for each treatment, $p < 0.05$).

(G) Preparation and recycling of wood-based panels.

(H and I) MOE (H) and MOR (I) of particleboards prepared from poplar wood particles and BSPI/Cys/Gly/St/CaP adhesives after three cycles (ANOVA, $N = 6$ for each treatment, $p < 0.05$).

(J and K) MOR and MOE of particleboards bonded with UF and PF adhesives after one cycle (ANOVA, $N = 6$ for each treatment, $p < 0.05$).

(L) Mechanism diagram of the recyclability in wood-based panels.

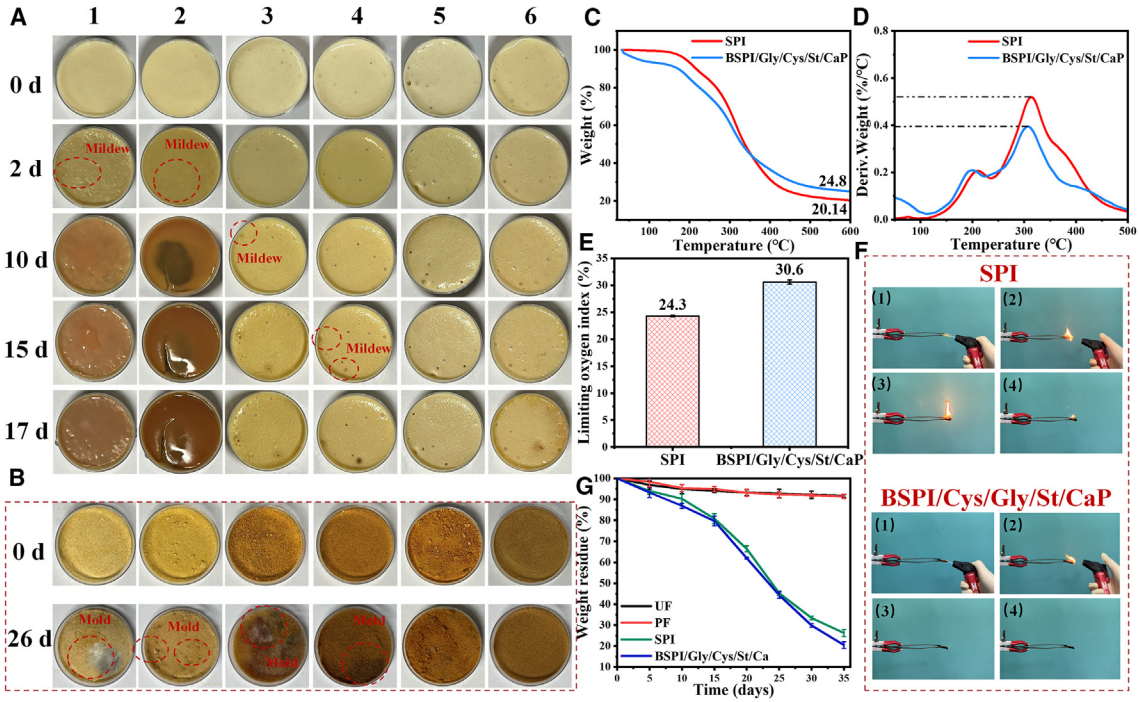

Figure 6. Additional properties of SP adhesives

(A and B) Images of mildew growth on (A) liquid and (B) cured SP adhesives (1: SPI, 2: BSPI, 3: BSPI/Cys, 4: BSPI/Cys/Gly, 5: BSPI/Cys/Gly/St, 6: BSPI/Cys/Gly/St/CaP).

(C–F) TG (C), derivative TG curves (D), limiting oxygen index values (E) (ANOVA, $N = 6$ for each treatment, $p < 0.05$), and (F) burning pictures of the SPI and BSPI/Cys/Gly/St/CaP adhesives.

(G) Weight residue profile of UF, PF, SPI, and BSPI/Cys/Gly/St/CaP adhesives after the degradation experiment (ANOVA, $N = 6$ for each treatment, $p < 0.05$).

contrast, particleboards bonded with UF and PF adhesives experienced a significant drop in MOR, with values falling to less than 20% of their initial values after only one cycle (Figures 5J and 5K). The reprocessability of particleboards prepared using the BSPI/Cys/Gly/St/CaP adhesive can be attributed to the heating and pressurization during the preparation process. These conditions promote dynamic bond exchange in the adhesive system, which causes the decomposition and reorganization of disulfide and borate ester bonds (Figure 5L). Additionally, the dynamic covalent bonds present act as sacrificial bonds, facilitating energy dissipation and stress transfer under external forces, thereby enhancing the mechanical properties and stability of the particleboard.[39]

Additional properties of SP adhesives

Biomass water-based adhesives are prone to degradation and deterioration caused by micro-organisms, leading to compromised bond strength and potential health risks.[40] To evaluate their resistance to mildew, samples of the SP adhesive were stored under constant temperature (30°C) and humidity (100% relative humidity) conditions in a controlled chamber. Liquid SPI and BSPI adhesive samples exhibited rapid mold growth (Figure 6A), with numerous small white colonies appearing on the adhesive surface within 2 days. However, the mildew resistance of the SP adhesives improved when Cys, Gly, St, and CaP were incorporated. The liquid BSPI/Cys/Gly/St/CaP adhesive did not show any color changes or mold growth even after 17 days, significantly extending the adhesive's pot life. Additionally, the mildew resistance of cured SP adhesives was evaluated. Except for BSPI/Cys/Gly/St and BSPI/Cys/Gly/St/CaP

adhesives, all cured adhesive samples exhibited mold growth within 26 days (Figure 6B). This improvement can be attributed to the synergistic enhancement of antifungal efficacy provided by Cys, Gly, and St,[30,41] which ensures the practical application of SP adhesives in harsh temperature and humidity conditions.

TG analysis was conducted to evaluate the thermal behavior of the adhesives. Compared to SPI, the residual mass of the BSPI/Cys/Gly/St/CaP adhesive increased from 20.14 to 24.8 wt %, while the thermal degradation rate decreased (Figures 6C and 6D). The limiting oxygen indices of the cured SPI adhesive and BSPI/Cys/Gly/St/CaP adhesive were measured as 24.3% and 30.6%, respectively (Figure 6E). Furthermore, the flame retardancy of these two adhesives, with identical sizes, was intuitively evaluated through burning tests. Figure 6F and Video S7 demonstrate that SPI continues to burn until complete combustion, whereas the BSPI/Cys/Gly/St/CaP adhesive ignites and then self-extinguishes (Video S8). These results indicate the improved thermal stability and flame retardancy of the BSPI/Cys/Gly/St/CaP adhesive, primarily due to the synergistic effect of abundant sulfur and the formation of a dense organic-inorganic composite system.[42,43]

The degradability of cured SPI, BSPI/Cys/Gly/St/CaP, and commercial adhesives (PF and UF) was assessed by burying them in natural soil (Figure 6G). No changes in mass were observed for petroleum-based PF and UF adhesives, whereas the SPI and BSPI/Cys/Gly/St/CaP adhesives underwent degradation, resulting in 26.21% and 20.47% of their original weights remaining, respectively, after 35 days of burial. Furthermore, the cured BSPI/Cys/Gly/St/CaP adhesive powder, mixed with soil at a 2:1 ratio, was used as soil for flowering plants such as Mozzie buster and sunflower. Successful germination of these plants occurred after an 8 day incubation period (Figure S9), indicating the environmentally friendly nature of the BSPI/Cys/Gly/St/CaP adhesive. Additionally, a life cycle assessment (LCA) was conducted to evaluate the environmental impact associated with the production of 1 kg of PF, UF, and BSPI/Cys/Gly/St/CaP adhesives (Table S1). The environmental impact of the BSPI/Cys/Gly/St/CaP adhesive was much lower than that of PF and UF adhesives, supporting the sustainable development and clean production of the adhesive industry.

In summary, we have developed a strong and reusable adhesive inspired by cutin, exhibiting excellent weather resistance comparable to that of commercial PF adhesives in accelerated aging tests. The adhesive effectively bonds various substrates, including wood, SS, glass, and Al, enabling SS sheets to pull a 1,135 kg car. Furthermore, the adhesive demonstrates outstanding reusability. The particleboard produced using the adhesive displays impressive mechanical properties, with an initial MOR of 19.25 MPa and an MOE of 3,133.05 MPa. Even after two cycles, the particleboard still meets the requirements for P2 particleboards (MOR > 11 MPa), outperforming UF and PF adhesives available in the market. Additionally, the adhesive exhibits resistance to mold (>17 days), flame retardancy (limiting oxygen index: 30.6%), degradability, and environmental friendliness. These attributes position it as a promising alternative to steel, plastic, and cement with biobased materials, accentuating their reprocessability. However, further research is required to comprehend the specific influence of different types of dynamic covalent bonds and the construction of strong and weak networks on adhesive performance. Our future goal is to investigate the mechanisms underlying the improved adhesive properties through the manipulation of dynamic covalent bond types and quantities. Additionally, exploring the room temperature curing of soy protein adhesives is essential to cater to a broader range of application scenarios, address diverse industrial requirements, and enhance the feasibility of adhesives on synthetic plastics.

Table 1. Detailed parameters for the preparation of adhesives

Adhesive samples	SPI (g)	Br (g)	EDC (g)	NHS (g)	Cys (g)	Gly (g)	St (g)	$CaCl_2$ (g)	H_3PO_4 (g)	Water (g)
SPI	15	–	–	–	–	–	–	–	–	70
BSPI	15	0.1	–	–	–	–	–	–	–	70
BSPI/Cys	15	0.1	0.45	0.12	3	–	–	–	–	66.43
BSPI/Cys/Gly	15	0.1	0.45	0.12	3	5	–	–	–	61.43
BSPI/Cys/Gly/St	15	0.1	0.45	0.12	3	5	0.6	–	–	60.83
BSPI/Cys/Gly/St/CaP	15	0.1	0.45	0.12	3	5	0.6	0.3	0.18	60.35
SPI/Cys/Gly/St/CaP	15	–	0.45	0.12	3	5	0.6	0.3	0.18	60.45

EXPERIMENTAL PROCEDURES

Resource availability

Lead contact

Further information and requests for resources and reagents should be directed to and will be fulfilled by the lead contact, Qiang Gao (gaoqiang@bjfu.edu.cn).

Materials availability

This study did not generate new unique reagents.

Data and code availability

- All data needed to evaluate the conclusions in the paper are present in the paper and supplemental information.
- Additional data related to this paper may be requested from the lead contact.

Chemicals

SPI with a protein content of 90%, Gly (96%), St (≥99%), N-(3-dimethylaminopropyl)-N′-ethylcarbodiimide hydrochloride (EDC; 98%), N-hydroxysuccinimide (NHS; 98%), Cys (99%), $CaCl_2$ (97%), H_3PO_4 (≥85%), potassium carbonate (K_2CO_3; 99%), sodium hydroxide (NaOH; 97%), PFs (E0 grade), UFs (E0 grade), bromelain, and poplar veneers were utilized without the need for further purification. Further detailed parametric information can be found in the supplemental information.

Synthesis of SP adhesives

A mixture of bromelain and SPI was dissolved in deionized water and stirred at 55°C for 10 min. The mixture was then moved into a water bath set at 100°C for 5 min to inactivate the bromelain, resulting in the enzymatically hydrolyzed SPI (BSPI) adhesive. NHS and EDC were dispersed in deionized water and added to the BSPI adhesive, followed by stirring for 15 min. Subsequently, Cys was added, and the mixture was stirred at 25°C for 6 h. Gly and St solutions were then introduced and stirred at 25°C for 20 min. The $CaCl_2$ solution and H_3PO_4 were sequentially added to the mixture to obtain the BSPI/Cys/Gly/St/CaP adhesive. The SPI, BSPI, BSPI/Cys, BSPI/Cys/Gly, BSPI/Cys/Gly/St, and SPI/Cys/Gly/St/CaP adhesives were prepared using the same concentrations and conditions as the BSPI/Cys/Gly/St/CaP adhesive (Table 1).

Characterization

Various analytical techniques were utilized to characterize the adhesives and their raw materials. Gel permeation chromatography, zeta potential analyzer, UV-vis, XPS, XRD, ATR-FTIR spectroscopy, Raman microscopy, SEM, EDS, TG analyzer, micro-scale combustion calorimeter, rheology, and LCA were employed for analysis. Detailed test methods can be found in the supplemental information.

Bond strength and lap shear tests

Bond strength tests were conducted to evaluate the shear strength of three-ply plywood bonded with the synthesized adhesives. Lap shear tests were performed to assess the adhesion between the adhesives and different substrates such as glass, wood, aluminum, and SS. Refer to the supplemental information for specific test methods.

Accelerated aging test of SP adhesives and plywood

Adhesive films of BSPI and BSPI/Cys/Gly/St/CaP were prepared by casting onto polytetrafluoroethylene sheets and allowing them to form films under specific conditions. Accelerated aging of the adhesives was performed by subjecting the cured adhesive films to boiling, freeze drying, and wet-heat aging cycles. ATR-FTIR and TG analysis were used to assess chemical structural changes and thermal stability. Detailed procedures are available in the supplemental information.

To evaluate the weather resistance of plywood bonded with SP adhesives, standardized testing methods such as BS EN 13986:2004 (BS1), BS EN 321:2002 (BS2), and GB/T17657-2013 (GB4-10) were used. These methods involve immersing the plywood specimens in water, boiling them, and subjecting them to cycles of freezing and drying. The shear strength of the specimens was then measured. Weather resistance of the adhesives was also evaluated using bond strength tests and cyclic residual rate tests. Further experimental details can be found in the supplemental information.

Preparation of particleboards and mechanical property tests

Residual rate tests were conducted on cured BSPI/Cys/Gly/St/CaP adhesive powder, which was soaked in deionized water, dried, and hot pressed. The resulting films were ground, and the residual rate was measured for multiple cycles.

The reusability of the BSPI/Cys/Gly/St/CaP film (SPI-based film) was evaluated by preparing new films from the ground powder and measuring the tensile strength and elastic modulus before and after the hot-press process.

The reprocessability of particleboards was assessed by breaking down previously prepared particleboards and adding water for subsequent hot pressing. The MOR and MOE were measured to determine the mechanical properties of the particleboards. UF-I, PF-I, UF-II, and PF-II were used as comparison materials. More specifics on the test methods can be found in the supplemental information.

Antimildew property tests

The resultant adhesives were loaded into Petri dishes and stored at 30°C with 100% relative humidity, and visual and olfactory observations were made daily to monitor any changes.

MD simulation

To explore the adhesion mechanism of the BSPI/Cys/Gly/St/CaP adhesive, MD simulations were conducted using the Materials Studio 2019 software program to investigate the adhesion and cohesion during the adhesive bonding process. More specifics on the test methods can be found in the supplemental information.

SUPPLEMENTAL INFORMATION

Supplemental information can be found online at https://doi.org/10.1016/j.xcrp.2024.102024.

ACKNOWLEDGMENTS

The financial support for this research was provided by the National Key R&D Program of China (2023YFD2201404), China; the National Natural Science Foundation of China (grant nos. 32071702 and 31722011), China; and the Engineering Research & Innovation Team Project of Beijing Forestry University (no. BLRC2023A02), China.

AUTHOR CONTRIBUTIONS

X.H. conceived and designed the experiments. X.H., Y.C., and X.L. conducted the synthesis and characterization. X.H. analyzed the data and generated figures. Jingchao Li and Jing Luo contributed to data processing and visualization. X.H. wrote the paper. P.S., Jianzhang Li, and Q. G. supervised this project. All authors discussed the results and commented on the manuscript.

DECLARATION OF INTERESTS

The authors declare no competing interests.

Received: February 26, 2024
Revised: April 16, 2024
Accepted: May 14, 2024
Published: June 5, 2024

REFERENCES

1. Bal-Ozturk, A., Cecen, B., Avci-Adali, M., Topkaya, S.N., Alarcin, E., Yasayan, G., Ethan, Y.C., Bulkurcuoglu, B., Akpek, A., Avci, H., et al. (2021). Tissue adhesives: From research to clinical translation. Nano Today *36*, 101049. https://doi.org/10.1016/j.nantod.2020.101049.

2. Chen, J., Dong, Z., Li, M., Li, X., Chen, K., and Yin, P. (2022). Ultra-Strong and Proton Conductive Aqua-Based Adhesives from Facile Blending of Polyvinyl Alcohol and Tungsten Oxide Clusters. Adv. Funct. Mater. *32*, 2111892. https://doi.org/10.1002/adfm.202111892.

3. Mu, C., Wang, X., Ma, Z., Liu, X., and Li, W. (2022). Redox and conductive underwater adhesive: an innovative electrode material for convenient construction of flexible and stretchable supercapacitors. J. Mater. Chem. A Mater. *10*, 7207–7217. https://doi.org/10.1039/D1TA10603A.

4. Jojibabu, P., Zhang, Y.X., and Prusty, B.G. (2020). A review of research advances in epoxy-based nanocomposites as adhesive materials. Int. J. Adhes. Adhes. *96*, 102454. https://doi.org/10.1016/j.ijadhadh.2019.102454.

5. Bekhta, P., Sedliačik, J., Noshchenko, G., Kačík, F., and Bekhta, N. (2021). Characteristics of beech bark and its effect on properties of UF adhesive and on bonding strength and formaldehyde emission of plywood panels. Eur. J. Wood Prod. *79*, 423–433. https://doi.org/10.1007/s00107-020-01632-8.

6. Sun, J., Han, J., Wang, F., Liu, K., and Zhang, H. (2022). Bioengineered Protein-based Adhesives for Biomedical Applications. Chem. Eur J. *28*, e202102902. https://doi.org/10.1002/chem.202102902.

7. Chen, Y., Meng, J., Gu, Z., Wan, X., Jiang, L., and Wang, S. (2020). Bioinspired Multiscale Wet Adhesive Surfaces: Structures and Controlled Adhesion. Adv. Funct. Mater. *30*, 1905287. https://doi.org/10.1002/adfm.201905287.

8. Stie, M.B., Kalouta, K., da Cunha, C.F.B., Feroze, H.M., Vetri, V., and Foderà, V. (2022). Sustainable strategies for waterborne electrospinning of biocompatible nanofibers based on soy protein isolate. Sustainable Materials and Technologies *34*, e00519. https://doi.org/10.1016/j.susmat.2022.e00519.

9. Periyasamy, A.P. (2022). Natural dyeing of cellulose fibers using syzygium cumini fruit extracts and a bio-mordant: A step toward sustainable dyeing. Sustainable Materials and Technologies *33*, e00472. https://doi.org/10.1016/j.susmat.2022.e00472.

10. Hao, Z., Xi, X., Hou, D., Lei, H., Li, C., Xu, G., and Du, G. (2023). A fully bio-based soy protein wood adhesive modified by citric acid with high water tolerance. Int. J. Biol. Macromol. *253*, 127135. https://doi.org/10.1016/j.ijbiomac.2023.127135.

11. Cui, Z., Xu, Y., Sun, G., Peng, L., Li, J., Luo, J., and Gao, Q. (2023). Improving Bond Performance and Reducing Cross-Linker Dosage of Soy Protein Adhesive via Hyper-Branched and Organic–Inorganic Hybrid Structures. Nanomaterials *13*, 203. https://doi.org/10.3390/nano13010203.

12. Zhang, J., Long, C., Zhang, X., Liu, Z., Zhang, X., Liu, T., Li, J., and Gao, Q. (2022). An easy-coating, versatile, and strong soy flour adhesive via a biomineralized structure combined with a biomimetic brush-like polymer. Chem. Eng. J. *450*, 138387. https://doi.org/10.1016/j.cej.2022.138387.

13. Huang, X., Cai, L., Li, Y., Liu, Q., Li, J., Li, J., and Gao, Q. (2023). Improving coating and prepressing performance of soy protein-based adhesive by constructing a dual-bionic topological structure. J. Clean. Prod. *384*, 135572. https://doi.org/10.1016/j.jclepro.2022.135572.

14. Xu, Y., Han, Y., Li, Y., Li, J., Li, J., and Gao, Q. (2022). Preparation of a strong, mildew-resistant, and flame-retardant biomimetic multifunctional soy protein adhesive via the construction of an organic-inorganic hybrid multiple-bonding structure. Chem. Eng. J. *437*, 135437. https://doi.org/10.1016/j.cej.2022.135437.

15. Huang, X., Chen, Y., Li, J., Li, J., Gao, Q., and Zhan, X. (2022). Improving the coating and prepressing properties of soybean meal adhesive by constructing a biomimetic topological structure. Mater. Des. *223*, 111163. https://doi.org/10.1016/j.matdes.2022.111163.

16. Atif, M., Ali, B., Imran, M., Riaz, N.N., Abdullah, M., Ahmad, M.H., and Mehmood, R.A. (2024). Synthesis and characterization of sesame oil based plasticizers for reversible bonding in thermally detachable polyurethane adhesives. Sustainable Materials and Technologies *39*, e00793. https://doi.org/10.1016/j.susmat.2023.e00793.

17. Szewciw, L.J., de Kerckhove, D.G., Grime, G.W., and Fudge, D.S. (2010). Calcification provides mechanical reinforcement to whale baleen α-keratin. Proc. Biol. Sci. *277*, 2597–2605. https://doi.org/10.1098/rspb.2010.0399.

18. Wang, B., Yang, W., McKittrick, J., and Meyers, M.A. (2016). Keratin: Structure, mechanical properties, occurrence in biological organisms, and efforts at bioinspiration. Prog. Mater. Sci. *76*, 229–318. https://doi.org/10.1016/j.pmatsci.2015.06.001.

19. McKittrick, J., Chen, P.Y., Bodde, S.G., Yang, W., Novitskaya, E.E., and Meyers, M.A. (2012).

The Structure, Functions, and Mechanical Properties of Keratin. JOM *64*, 449–468. https://doi.org/10.1007/s11837-012-0302-8.

20. Ashby, M.F., Gibson, L.J., Wegst, U., and Olive, R. (1997). The mechanical properties of natural materials. I. Material property charts. Proceedings of the Royal Society of London. Series A: Mathematical and Physical Sciences *450*, 123–140. https://doi.org/10.1098/rspa.1995.0075.

21. Duan, H., Li, K., Xie, M., Chen, J.M., Zhou, H.G., Wu, X., Ning, G.H., Cooper, A.I., and Li, D. (2021). Scalable Synthesis of Ultrathin Polyimide Covalent Organic Framework Nanosheets for High-Performance Lithium-Sulfur Batteries. J. Am. Chem. Soc. *143*, 19446–19453. https://doi.org/10.1021/jacs.1c08675.

22. Liu, B., Zhao, F., Qiu, Y., Liu, W., and Wu, Z. (2023). A cysteamine-functionalized biomimetic chromotropic hydrogel for naked-eye detection and adsorption of mercury ions. J. Mater. Chem. C Mater. *11*, 1499–1508. https://doi.org/10.1039/D2TC04234G.

23. Chu, K., Li, X., Li, Q., Guo, Y., and Zhang, H. (2021). Synergistic Enhancement of Electrocatalytic Nitrogen Reduction Over Boron Nitride Quantum Dots Decorated Nb2CTx-MXene. Small *17*, 2102363. https://doi.org/10.1002/smll.202102363.

24. Chen, F., Chen, D., Deng, T., and Li, J. (2022). Combination of alkaline phosphatase/graphene oxide nanoconjugates and D-glucose-6-phosphate–functionalized gold nanoparticles for the rapid colorimetric assay of pathogenic bacteria. Biosens. Bioelectron. *216*, 114611. https://doi.org/10.1016/j.bios.2022.114611.

25. Zhao, Z.-H., Zhao, P.-C., Zhao, Y., Zuo, J.-L., and Li, C.-H. (2022). An Underwater Long-Term Strong Adhesive Based on Boronic Esters with Enhanced Hydrolytic Stability. Adv. Funct. Mater. *32*, 2201959. https://doi.org/10.1002/adfm.202201959.

26. Chen, Y., Zhang, Y., Chen, X., Huang, J., Zhou, B., Zhang, T., Yin, W., Fang, C., Yin, Z., Pan, H., et al. (2023). Biomimetic Intrafibrillar Mineralization of Native Tendon for Soft–Hard Interface Integration by Infiltration of Amorphous Calcium Phosphate Precursors. Adv. Sci. *10*, 2304216. https://doi.org/10.1002/advs.202304216.

27. Chen, L., Gao, Q., Zhang, J., Chen, H., Zhang, S., and Li, J. (2014). Effects of Assembly Time on Wet Shear Strength and Formaldehyde Emission of Plywood Bonded by Urea Formaldehyde Resin. Bioresources *9*. https://doi.org/10.15376/biores.9.2.2975-2986.

28. Xu, Y., Huang, X., Zhang, Y., Liu, Z., Luo, J., Li, J., Li, J., and Gao, Q. (2021). A high bonding performance and antibacterial soybean meal adhesive with Maillard reaction based cross-linked structure. Compos. B Eng. *227*, 109403. https://doi.org/10.1016/j.compositesb.2021.109403.

29. Zhang, Y., Liu, Z., Xu, Y., Li, J., Shi, S.Q., Li, J., and Gao, Q. (2021). High performance and multifunctional protein-based adhesive produced via phenol-amine chemistry and mineral reinforcement strategy inspired by arthropod cuticles. Chem. Eng. J. *426*, 130852. https://doi.org/10.1016/j.cej.2021.130852.

30. Gu, W., Li, F., Liu, X., Gao, Q., Gong, S., Li, J., and Shi, S.Q. (2020). Borate chemistry inspired by cell walls converts soy protein into high-strength, antibacterial, flame-retardant adhesive. Green Chem. *22*, 1319–1328. https://doi.org/10.1039/C9GC03875B.

31. Chen, C., Chen, F., Liu, B., Du, Y., Liu, C., Xin, Y., and Liu, K. (2019). Peanut meal-based wood adhesives enhanced by urea and epichlorohydrin. R. Soc. Open Sci. *6*, 191154. https://doi.org/10.1098/rsos.191154.

32. Xi, X., Pizzi, A., Frihart, C.R., Lorenz, L., and Gerardin, C. (2020). Tannin plywood bioadhesives with non-volatile aldehydes generation by specific oxidation of mono- and disaccharides. Int. J. Adhes. Adhes. *98*, 102499. https://doi.org/10.1016/j.ijadhadh.2019.102499.

33. Chen, X., Xi, X., Pizzi, A., Fredon, E., Du, G., Gerardin, C., and Amirou, S. (2021). Oxidized demethylated lignin as a bio-based adhesive for wood bonding. J. Adhes. *97*, 873–890. https://doi.org/10.1080/00218464.2019.1710830.

34. Zhang, J., Liu, B., Zhou, Y., Essawy, H., Chen, Q., Zhou, X., and Du, G. (2021). Preparation of a starch-based adhesive cross-linked with furfural, furfuryl alcohol and epoxy resin. Int. J. Adhes. Adhes. *110*, 102958. https://doi.org/10.1016/j.ijadhadh.2021.102958.

35. Liang, K., Zhao, C., Song, C., Zhao, L., Qiu, P., Wang, S., Zhu, J., Gong, Z., Liu, Z., Tang, R., et al. (2023). In Situ Biomimetic Mineralization of Bone-Like Hydroxyapatite in Hydrogel for the Acceleration of Bone Regeneration. ACS Appl. Mater. Interfaces *15*, 292–308. https://doi.org/10.1021/acsami.2c16217.

36. Li, X., Lai, J., Deng, Y., Song, J., Zhao, G., and Dong, S. (2020). Supramolecular Adhesion at Extremely Low Temperatures: A Combined Experimental and Theoretical Investigation. J. Am. Chem. Soc. *142*, 21522–21529. https://doi.org/10.1021/jacs.0c10786.

37. Zhang, Q., Wang, W., Cai, C., Wu, S., Li, J., Li, F., and Dong, S. (2022). Underwater luminescent labeling materials constructed from a supramolecular approach. Mater. Horiz. *9*, 1984–1991. https://doi.org/10.1039/D2MH00211F.

38. Gu, W., Liu, X., Ye, Q., Gao, Q., Gong, S., Li, J., and Shi, S.Q. (2020). Bio-inspired co-deposition strategy of aramid fibers to improve performance of soy protein isolate-based adhesive. Ind. Crop. Prod. *150*, 112424. https://doi.org/10.1016/j.indcrop.2020.112424.

39. Tratnik, N., Tanguy, N.R., and Yan, N. (2023). Recyclable, self-strengthening starch-based epoxy vitrimer facilitated by exchangeable disulfide bonds. Chem. Eng. J. *451*, 138610. https://doi.org/10.1016/j.cej.2022.138610.

40. Lu, P., Guo, L., Wang, Z., Li, B., Li, J., Li, Y., Qiu, D., Shi, W., Yang, L., Wang, N., et al. (2020). A rare gain of function mutation in a wheat tandem kinase confers resistance to powdery mildew. Nat. Commun. *11*, 680. https://doi.org/10.1038/s41467-020-14294-0.

41. Xu, C., Xu, Y., Chen, M., Zhang, Y., Li, J., Gao, Q., and Shi, S.Q. (2020). Soy protein adhesive with bio-based epoxidized daidzein for high strength and mildew resistance. Chem. Eng. J. *390*, 124622. https://doi.org/10.1016/j.cej.2020.124622.

42. Kim, N.K., Bruna, F.G., Das, O., Hedenqvist, M.S., and Bhattacharyya, D. (2020). Fire-retardancy and mechanical performance of protein-based natural fibre-biopolymer composites. Composites Part C: Open Access *1*, 100011. https://doi.org/10.1016/j.jcomc.2020.100011.

43. Wicklein, B., Kocjan, D., Carosio, F., Camino, G., and Bergström, L. (2016). Tuning the Nanocellulose–Borate Interaction To Achieve Highly Flame Retardant Hybrid Materials. Chem. Mater. *28*, 1985–1989. https://doi.org/10.1021/acs.chemmater.6b00564.